DIFFERENCES AND SIMILARITIES IN THE PROCESSING OF AIRBORNE AND SPACEBORNE HYPERSPECTRAL DATA SHOWN ON HYSPEX AND ENMAP PROCESSING CHAINS

Mathias Schneider, Andreas Baumgartner, Peter Schwind, Emiliano Carmona, Tobias Storch

German Aerospace Center (DLR), Remote Sensing Technology Institute (IMF), Münchener Str. 20, 82234 Weßling, Germany

ABSTRACT

When working with hyperspectral data, it is very important, that the data is properly pre-processed in terms of systematic radiometric and spectral correction, geometric correction as well as atmospheric correction. Airborne and spaceborne sensors show some similarities regarding the processing, but also some differences. In this paper, these similarities and differences are discussed on the example of the HySpex processing chain in the generic processing environment Catena and the EnMAP processor that is currently developed at DLR. The paper presents the different sensors and their properties and gives an overview of the different workflows and the used algorithms.

Index Terms— Hyperspectral, EnMAP, HySpex

1. INTRODUCTION

Pre-processing is an essential step before analyzing the actual content of any EO data. Usually, the pre-processing of hyperspectral data consists of applying the spectral/radiometric calibration to the data (level 1B processing), the geometric correction (level 1C processing) and the atmospheric correction (level 2A processing). In most cases, the pre-processing is realized by automatic processing chains. This applies to data of both airborne and spaceborne sensors. Can similar processing chains be used for the processing of hyperspectral data from airborne and spaceborne sensors? In this paper, the processing chains for HySpex and EnMAP data are presented to allow for a comparison.

2. THE SENSORS

2.1. HySpex

In 2011, the Remote Sensing Technology Institute (IMF) of the German Aerospace Center (DLR) purchased an airborne imaging spectrometer system with the intention to investigate potential earth observation applications for the German satellite mission EnMAP from the Norwegian Company Norsk Elektro Optikk A/S (NEO). The System features two different cameras covering the VNIR and SWIR spectral domain. Both cameras have been extensively characterized at IMF in cooperation with the National German Metrology Institute (PTB), resulting in a very well characterized high precision instrument suited for benchmark earth observation applications. Due to the high spatial and spectral resolution, the system is mainly used for feasibility studies and for the validation of satellite measurements. The HySpex system is also available to external customers and research facilities via the user service OpAiRS. The HySpex VNIR-1600 features a CCD detector covering the spectral range 416−992 nm with 160 channels. This results in a spectral sampling interval of 3.6 nm. The spectral resolution ranges from 3.5 nm at nadir to approximately 6 nm at the outer edge of the swath. The HySpex SWIR-320m-e is equipped with a mercury cadmium telluride (MCT) detector with 256 channels covering the spectral range 968−2498 nm at a sampling interval of 6 nm and a spectral resolution of 5.6−7.0 nm. The VNIR detector has a width of 1600 pixels while the SWIR detector has a width of 320 pixels. As is the case for every airborne sensor, the spatial resolution is depending on the flight height. More information on the HySpex sensors can be found in [1].

2.2. EnMAP

The imaging spectroscopy remote sensing mission EnMAP (Environmental Mapping and Analysis Program, enmap.org) will fill the gap in space-based imaging spectroscopy products [2]. The mission relies on a prism-based dual-spectrometer [3]. The VNIR spectrometer covers the spectral range from 420 nm to 1000 nm with a spectral sampling distance between 4.8 nm and 8.2 nm. The SWIR spectrometer covers the spectral range from 900 nm to 2450 nm with a spectral sampling distance between 7.4 nm and 12.0 nm. A signal-to-noise ratio at reference radiance level of 500:1 at 495 nm and 150:1 at 2200 nm is achieved, with a radiometric resolution of 14 bits. Each detector array has 1000 valid pixels in spatial direction with an instantaneous field-of-view of 9.5 arcsec, this results in a geometric resolution of 30 m × 30 m and a swath width (across-track) of 30 km. A swath length (along-track) of 5000 km can be acquired per day and a target revisit time of less than 4 days is enabled by an across-track tilt capability of 30°. It is remarked that the two 2-dimensional detector arrays are not

spatially aligned, namely there is a shift of approximately 190 arcsec along track which corresponds to approximately 600 m on ground. A spectral accuracy of better than 0.5 nm in VNIR and 1.0 nm in SWIR as well as a radiometric accuracy of better than 5% is achieved. A geometric accuracy of 100 m is achieved, improved by on-ground processing to 30 m with respect to a used reference image. The launch is scheduled for 2020 with an operational lifetime of 5 years. The hyperspectral image products at different processing levels will be freely available to the scientific user community for measuring and analyzing bio-, geochemical, and physical parameters characterizing the Earth's surface. The OHB System AG is responsible for realizing the space segment and the Earth Observation Center (EOC), together with the German Space Operations Center (GSOC), of the German Aerospace Center (DLR) is responsible for establishing and operating the ground segment [4]. Mission management is covered by the DLR Space Administration.

3. SPECTRAL/RADIOMETRIC CALIBRATION

3.1. HySpex

Being an airborne sensor, HySpex benefits from the possibility of an extensive, regularly performed characterization in the Calibration Home Base at DLR [5]. The obtained characterization is then used in the level 1B processing described in the section 5 of this paper. Details on the calibration can be found in [6].

3.2. EnMAP

Being a spaceborne sensor, EnMAP can only be characterized in a laboratory before the launch. In orbit, various calibration measurements are used to provide a valid set of calibration tables. The most frequent calibration measurements are the dark current measurements which are taken before and after each datatake. The onboard calibration assembly consists of a main sphere coated inside with white spectralon® and different light sources (LEDs, and halogen lamps) and of a sphere with doped spectralon® for spectral calibration purposes. For the absolute radiometric calibration, sun calibration is used. Details on the calibration methods can be found in [7].

4. GEOMETRY

4.1. HySpex

The interior orientations of the two sensors are stable and are characterized in the regular laboratory calibration. However, each time that the sensors are installed in the planes, the mounting angles, i.e. the angles between the VNIR/SWIR sensors and the IMU, are different. Due to the high spatial resolution, reference images with an appropriate accuracy are usually not available for the processing. Therefore, at the beginning of each campaign, images over an area at Kaufbeuren are acquired, where high quality reference images are available. For this dataset, the mounting angles are estimated using image matching techniques. These mounting angles are then considered as valid and are used in the processing chain as long as the installation of the HySpex system doesn't change.

4.2. EnMAP

Before launch, the geometry of the EnMAP instruments will be extensively characterized in the laboratory. In orbit, geometric calibration will be performed regularly using reference images and image matching techniques. This allows for a geolocation accuracy of 100 m which will be improved during processing by using a global reference database, most probably consisting of Sentinel-2 images, and image matching techniques.

5. PROCESSING CHAINS

5.1. HySpex

The HySpex processing chain consists of two parts: The preparation of the data for the automatic processing consists of processing of GPS and IMU data and assigning them to the corresponding flight strips. The second part, consisting of systematic correction, orthorectification, co-registration and atmospheric correction is realized in the generic processing system Catena, developed at DLR [8]. The workflow is shown in figure 1.

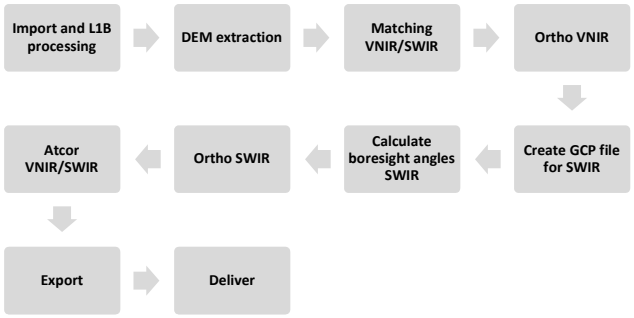

Figure 1: Processing chain for HySpex data in Catena

The first step in Catena processing chains is always the import of the data from the specific sensor format to the generic Catena format. In case of HySpex, this is combined with the level 1B processing. Therefore, the following steps are applied on each frame in the given order: Dark signal correction, linearity correction (VNIR only), stray light correction (VNIR only), radiometric calibration, bad pixel correction (SWIR only) and finally correction of point spread function (PSF) non-uniformities.

The linearity correction of the VNIR instrument is performed after the dark signal correction, since the dark current is very stable and does not significantly change. For the stray light correction, a four dimensional tensor is applied [9]. Currently, only the VNIR data are corrected for stray light, while the measurement of the SWIR instrument's stray light is currently ongoing research. The radiometric calibration is performed by dividing the signal corrected to this point by the radiometric response multiplied by the

integration time. The radiometric responses of both instruments are determined during laboratory calibration and are traceable to système international (SI) units via the German metrology institute Physikalisch-Technische Bundesanstalt (PTB) [6]. The bad pixels of the HySpex SWIR are corrected by linear interpolation between adjacent pixels along the spectral axis, while the bad pixels of the VNIR are corrected by the camera software. Finally, optical distortions like smile, keystone and - equally important - the individual angular and spectral resolutions of each pixel are corrected by applying an individual homogenization kernel on each pixel.

The next step is the extraction of a DEM from a DEM database, e.g. SRTM. Then tie points between VNIR in SWIR data are found in bands located in the overlapping spectral domain using a BRISK matching. [10] After this step, the VNIR image is orthorectified using the physical sensor model, the GPS-/IMU-data, the previously obtained mounting angles and the DEM by the DLR software ORTHO. The tie points are inserted as check points (CPs) to obtain the respective geo-coordinates. From these geo-coordinates and the original SWIR image coordinates, a ground control point (GCP) file is created for the SWIR images that is used in the DLR software ESTIMATE to estimate the boresight angles for the SWIR image relatively to the VNIR image. Using these boresight angles, the SWIR image is then orthorectified, thus assuring a high co-registration accuracy. In the next step, ATCOR [11] is used for the atmospheric correction. The last steps are standard steps for each processing chain in Catena and consist of converting the images from the generic format to the requested output format, e.g. ENVI or geotiff, and copying it to the defined output directory.

5.2. EnMAP

The EnMAP processing chain consists of mostly new developments and some existing modules, especially in the geometric processing. It generates fully-automatic standardized high-quality products at different levels for the international scientific users. Operational data quality control, namely a quantitative assessment of various properties, are provided for each processing step to account for the demand in highly reliable, well documented and standardized data products. By this process the valid function of the sensor and processing chain is investigated and thus ensured.

The Level 0 processor generates time-tagged instrument raw data with auxiliary information which are long-term archived, but not distributed to the users. Therefore, unpacking, decompression, screening, dark current extraction, and tiling to areas of about 30 km × 30 km is performed. Afterwards, Level 1B, 1C, and 2A processing is performed to finally generate consistent metadata and quicklooks.

The Level 1B processor generates TOA radiances, not resampled, spectrally and geometrically characterized, radiometrically calibrated, and annotated, e.g. with pixel classification (usability mask) and information necessary for later processing. Therefore, defective pixel flagging, nonlinearity correction, dark signal (and digital offset) correction, gain matching, straylight correction, radiometric/spectral referencing, radiometric calibration, and spectral defective pixel interpolation (using a simplified pixel-based atmospheric correction) is performed. Although thematically located in the L1C processor, some parts of the geometric processing are already performed in the L1B processor to provide essential parameters/metadata for the following steps. This includes the establishment of GCPs using image matching techniques and a reference image database and DEM to obtain a robust sensor model refinement for the complete acquisition and for generating the rational polynomial coefficients (RPC).

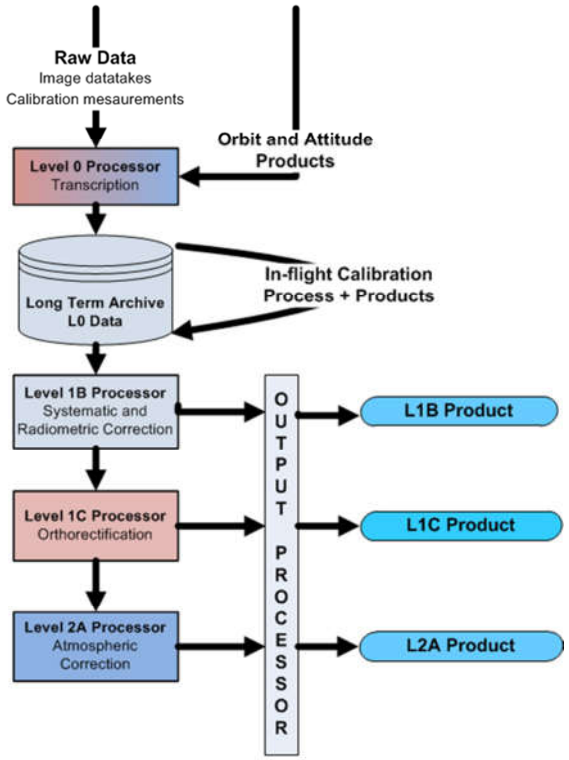

Figure 2: EnMAP processing chain

The Level 1C processor orthorectifies Level 1B products to a user selected map projection (UTM, geographic, or European projection LAEA) using a user selected resampling method (nearest neighbor, bi-linear interpolation, or cubic convolution). As for HySpex, the DLR software ORTHO is used taking into account the physical sensor model, with a correction of sensor interior orientation, satellite motion, light aberration and refraction, and terrain related distortions.

The Level 2A processor applies an atmospheric correction with different methods over land and water areas to Level 1C products resulting in orthorectified BOA reflectances.

Therefore, a classification (land-water-background, cloud, shadow, haze, cirrus, snow, Sun glitter), cirrus (and for land also haze) removal which depends on user selection, aerosol optical thickness (and for land also columnar water vapor) estimation is performed to obtain surface or subsurface reflectances including an adjacency correction. The six atmospheric functions path radiance, direct and diffuse transmittance ground-to-sensor, direct and diffuse solar flux, and spherical albedo are considered.
Level 1B, 1C, and 2A products are generated to a user selected format (image data in BSQ, BIL, BIP, JPEG2000, or GeoTIFF and metadata in XML) and disseminated through web-based interfaces.

6. ASSESSMENT

The processing chains are quite similar. In the L1B processing, data in both processing chains are corrected for dark signal, non-linearity, stray light, bad pixels and the radiometric calibration is applied. The algorithms used for this task are partly different due to the different design of the instruments. Regarding the geometric processing, there are some slight differences: EnMAP data are, if possible, matched to reference images to improve the geometric accuracy, whereas HySpex data are only matched at the beginning of a campaign and the resulting mounting angles are considered stable for the whole campaign. For the orthorectification itself, the same software is used. For the atmospheric correction, i.e. L2A processing, the only difference is the use of different algorithms over land and water in the EnMAP processing chain.

6. CONCLUSION

The processing chains for data from airborne and spaceborne sensors are quite similar; some software modules are even used in both chains. The main differences can be found in the design of the processing chains, but this is mainly caused by the different requirements for the respective products. Also some algorithms especially in the L1B processing are different due to the different design of the sensors. Nevertheless, both processing chains have profited from each other. The experiences made with HySpex supported the development of the EnMAP chain while some parts of the ENMAP chain, e.g. the derivation of quality parameters, will find their way into the HySpex chain in the future.

8. ACKNOWLEDGEMENTS

Supported by the DLR Space Administration with funds of the German Federal Ministry of Economic Affairs and Technology on the basis of a decision by the German Bundestag (50 EE 0850).

11. REFERENCES

[1] C. Köhler, “Airborne Imaging Spectrometer HySpex”. *Journal of Large-Scale Research Facilities JLSRF, 2 (A93), pp. 1-6.* Forschungszentrum Jülich GmbH. doi: 10.17815/jlsrf-2-151, 2016

[2] L. Guanter, H. Kaufmann, K. Segl, S. Foerster, C. Rogass, S. Chabrillat, T. Kuester, A. Hollstein, G. Rossner, C. Chlebek, C. Straif, S. Fischer, S. Schrader, T. Storch, U. Heiden, A. Müller, M. Bachmann, H. Mühle, R. Müller, M. Habermeyer, A. Ohndorf, J. Hill, H. Buddenbaum, P. Hostert, S. van der Linden, P.J. Leitao, A. Rabe, R. Doerffer, H. Krasemann, H. Xi, W. Mauser, T. Hank, M. Locherer, M. Rast, K. Staenz, and B. Sang, “The EnMAP spaceborne imaging spectroscopy mission for Earth observation”, *Remote Sensing*, *vol. 7, no. 7, pp. 8830*, 2015.

[3] H. Kaufmann, B. Sang, T. Storch, K. Segl, S. Foerster, L. Guanter, M. Erhard, B. Heider, S. Hofer, H.-P. Honold, B. Penné, M. Bachmann, M. Habermeyer, A. Müller, R. Müller, M. Rast, K. Staenz, C. Straif, and C. Chlebek, “Environmental Mapping and Analysis Program – A German Hyperspectral Mission”, *Optical Payloads for Space Missions*, *pp. 161–182*, 2016.

[4] T. Storch, M. Habermeyer, S. Eberle, H. Mühle, and R. Müller, “Towards a Critical Design of an Operational Ground Segment for an Earth Observation Mission”, *Journal of Applied Remote Sensing*, vol. 7, *no. 1, pp. 1–12*, 2013.

[5] J. Brachmann, A. Baumgartner and P. Gege, “The Calibration Home Base for Imaging Spectrometers”, *Journal of Large-Scale Research Facilities JLSRF, 2 (A82), pp. 1-9*. Forschungszentrum Jülich, Central Library. DOI: 10.17815/jlsrf-2-137, 2016.

[6] K. Lenhard, A. Baumgartner, and T. Schwarzmaier, “Independent laboratory characterization of NEO HySpex imaging spectrometers vnir-1600 and swir-320m-e", *Geoscience and Remote Sensing, IEEE Transactions on 53(4), pp. 1828-1841,* 2015.

[7] H. Krawczyk, B. Gerasch, T. Walzel, T. Storch, R. Müller, B. Sang, and C. Chlebek, “EnMAP Radiometric Inflight Calibration”, *Proceedings of IEEE International Geoscience and Remote Sensing Symposium (IGARSS) 2014 (4132), pp. 1-5,* 2014.

[8] T. Krauß, P. d'Angelo, M. Schneider and V. Gstaiger, “The Fully Automatic Optical Processing System CATENA at DLR”, *ISPRS Int. Arch. Photogramm. Remote Sens. Spatial Inf. Sci., XL-1/W, pp. 177-181, Copernicus Publication, ISPRS Hannover Workshop,* doi: 10.5194/isprsarchives-XL-1-W1-177-2013, 2013

[9] K. Lenhard, A. Baumgartner, P. Gege, S. Nevas, S. Nowy and A. Sperling, “Impact of improved calibration of a NEO HySpex VNIR-1600 sensor on remote sensing of water depth”, *IEEE Transactions on Geoscience and Remote Sensing, 53 (11), pp. 6085-609,*.IEEE - Institute of Electrical and Electronics Engineers. doi: 10.1109/TGRS.2015.2431743, 2015

[10] P. Schwind, M. Schneider and R. Müller, “Improving HySpex Sensor Co-Registration Accuracy using BRISK and Sensor-model based RANSAC”, *Pecora 19 Symposium in conjunction with the Joint Symposium of ISPRS Technical Commission I and IAG Commission 4 (Vol. XL-1, pp. 371–376), ISPRS Archive,* doi: 10.5194/isprsarchivesXL-1-371-2014, 2014

[11] R. Richter, “Correction of satellite imagery over mountainous terrain”, *Appl. Opt., 37(18), pp. 4004–4015,* 1998